

ornl

**OAK RIDGE
NATIONAL
LABORATORY**

MARTIN MARIETTA

MARTIN MARIETTA ENERGY SYSTEMS LIBRARIES



3 4456 0262429 3

ORNL/TM-10403

Effect of Infiltration Conditions on the Properties of SiC/Nicalon Composites

R. A. Lowden
A. J. Caputo
D. P. Stinton
T. M. Besmann
M. D. Morris

OAK RIDGE NATIONAL LABORATORY
CENTRAL RESEARCH LIBRARY
CIRCULATION SECTION
4500N ROOM 123
LIBRARY LOAN COPY
DO NOT TRANSFER TO ANOTHER PERSON
If you wish someone else to see this
report, send in name with report and
the library will arrange a loan.

OPERATED BY
MARTIN MARIETTA ENERGY SYSTEMS, INC.
FOR THE UNITED STATES
DEPARTMENT OF ENERGY

*Fossil
Energy
Program*

Printed in the United States of America. Available from
National Technical Information Service
U.S. Department of Commerce
5285 Port Royal Road, Springfield, Virginia 22161
NTIS price codes—Printed Copy: A03 Microfiche A01

This report was prepared as an account of work sponsored by an agency of the United States Government. Neither the United States Government nor any agency thereof, nor any of their employees, makes any warranty, express or implied, or assumes any legal liability or responsibility for the accuracy, completeness, or usefulness of any information, apparatus, product, or process disclosed, or represents that its use would not infringe privately owned rights. Reference herein to any specific commercial product, process, or service by trade name, trademark, manufacturer, or otherwise, does not necessarily constitute or imply its endorsement, recommendation, or favoring by the United States Government or any agency thereof. The views and opinions of authors expressed herein do not necessarily state or reflect those of the United States Government or any agency thereof.

Metals and Ceramics Division

EFFECT OF INFILTRATION CONDITIONS ON THE
PROPERTIES OF SiC/NICALON COMPOSITES

R. A. Lowden, A. J. Caputo, D. P. Stinton,
T. M. Besmann, and M. D. Morris

Date Published - May 1987

NOTICE: This document contains information of
a preliminary nature. It is subject to revision
or correction and therefore does not represent a
final report.

Research Sponsored by
the U.S. Department of Energy,
Advanced Research and Technology Development
Fossil Energy Materials Program

Prepared by the
OAK RIDGE NATIONAL LABORATORY
Oak Ridge, Tennessee 37831
operated by
MARTIN MARIETTA ENERGY SYSTEMS, INC.
for the
U.S. DEPARTMENT OF ENERGY
under Contract DE-AC05-84OR21400



3 4456 0262429 3

CONTENTS

ABSTRACT	1
INTRODUCTION	1
STATISTICAL DESIGN	2
EXPERIMENTAL	3
PROCESSING	3
TESTING	6
RESULTS	8
PROCESSING TIME	8
DENSITY	8
ROOM-TEMPERATURE FLEXURE STRENGTH	11
PROCESS RELATIONSHIPS	11
DISCUSSION	16
THERMODYNAMICS AND KINETICS	16
PRESSURE	19
TEMPERATURE	19
TOTAL FLOW RATE	20
HYDROGEN:MTS RATIO	20
CONCLUSIONS	21
ACKNOWLEDGMENTS	21
REFERENCES	22

EFFECT OF INFILTRATION CONDITIONS ON THE
PROPERTIES OF SiC/NICALON COMPOSITES*

R. A. Lowden, A. J. Caputo, D. P. Stinton,
T. M. Besmann, and M. D. Morris[†]

ABSTRACT

A statistically designed experiment was performed to evaluate the effects of process variables on fiber-reinforced SiC composites fabricated by chemical vapor infiltration. Response surface methodology was applied to study the influence of temperature, pressure, reactant supply rate, and gas ratios on the deposition process and the properties of the produced material. Deposition temperature and total gas flow rates had inverse effects on density and strength, while the effect of pressure was statistically insignificant. Low $H_2:CH_3SiCl_3$ ratios evoked a positive response in all dependent variables.

INTRODUCTION

Fiber-reinforced ceramic composites are being developed as potential candidates for high-temperature structural materials. High-strength ceramic fibers incorporated into brittle matrices prevent catastrophic failure by improving fracture toughness through energy dissipation processes such as fiber pull-out and crack deflection.¹⁻³ Ceramic composite systems exhibiting improved strength and fracture toughness over monolithic ceramics have been reported,⁴⁻⁶ but many of the conventional ceramic manufacturing techniques used to produce them tend to mechanically, thermally, or chemically damage the fibers. Procedures have been developed to fabricate fiber-reinforced ceramic composites by depositing a matrix within a fibrous structure using relatively low-temperature, low-stress chemical vapor deposition techniques,⁷ reducing fiber degradation.

*Research sponsored by the U.S. Department of Energy, AR&TD Fossil Energy Materials Program [DOE/FE AA 15 10 10 0, Work Breakdown Structure Element ORNL-1(A)] under contract DE-AC05-84OR21400 with Martin Marietta Energy Systems, Inc.

[†]Engineering Physics and Mathematics Division.

Termed chemical vapor infiltration, the technique has been applied to a variety of fiber-matrix combinations, which has resulted in material with favorable mechanical properties, but the process has been dependent on diffusion and thus involves long processing times.⁸⁻¹⁶ An improved infiltration process, reducing processing times from weeks to hours, has now been developed combining thermal-gradient and pressure-gradient approaches.¹⁷⁻²³

A major portion of our early investigations involved the infiltration of Nicalon* fibrous structures with SiC. Uniform deposition throughout cloth preforms was achieved utilizing the pyrolysis of methyltrichlorosilane (MTS or CH_3SiCl_3) in the presence of hydrogen with a furnace temperature of ~ 1475 K and atmospheric pressure. These conditions resulted in comparatively high-density composites exhibiting high strength and fracture toughness in completion times of less than 30 h for a 45-mm-diam \times 12.5-mm-thick disk sample.

The purpose of the study reported here was to analyze the combined effect of temperature, pressure, gas ratios and total gas flow on the thermal-gradient, pressure-gradient process as applied to the SiC/Nicalon system. Infiltration time, strength, and final density were selected as the initial response variables to be examined. The information obtained can be used to choose the optimum conditions required to achieve a final product with the highest density and strength and uniform infiltration in the shortest time.

STATISTICAL DESIGN

An experiment was statistically designed using response surface methods to study the effects of temperature, pressure, H_2 :MTS ratio, and total gas flow on various properties. Response surface methodology consists of a group of methods used in the empirical study of the relationships between one or more measured responses and a number of input variables.^{24,25} The methods were used to determine what sets of experimental variables are required to produce the best combination of strength, density, and uniform infiltration in the shortest time. The experimental

*Nippon Carbon Company, Tokyo, Japan.

parameters, temperature, pressure, total gas flow, and the volume ratio of H_2 :MTS, were statistically combined in a four-dimensional array utilizing a central composite design.²⁶

A minimum of 30 experimental sets of conditions were necessary to provide the required data to evaluate the contributions and interactions of the four factors. The nominal levels of the four experimental parameters are summarized in Table 1. The region to be explored is defined by the following minima and maxima; temperatures from 1375 to 1575 K, pressures from 10 to 100 kPa, total gas flows from 275 to 1100 cm^3/min , and H_2 :MTS from 10 to 35. The central point was placed at a temperature of 1475 K, a pressure of 55 kPa, a total gas flow of 550 cm^3/min and H_2 :MTS = 20:1. Four runs at the central point verified the reproducibility. Two points were added to assess the response of a higher-temperature value and of a lower H_2 :MTS ratio.

EXPERIMENTAL

PROCESSING

The experiments were carried out in a water-jacketed furnace resistively heated using a graphite element. The critical components of the infiltration apparatus, the water-cooled injector and the graphite holder, have been described previously.¹⁷⁻²³ A schematic of the system is shown in Fig. 1. Fibrous preforms are retained within a graphite holder that contacts a water-cooled metal gas distributor, thus cooling the bottom and side surfaces of the substrate. The top of the fibrous preform is exposed to the hot zone of the furnace, creating a steep temperature gradient across the preform. The reactant gases initially pass into the cooled area of the preform but do not react because of the low temperature. The gases continue from the cooled region of the preform into the hotter regions, where the MTS decomposes and SiC deposits on and around the fibers to form the matrix. When the top surface becomes coated and is no longer permeable, the gases flow radially through the substrate to the preform circumference and exit through the perforated retaining lid.

The gas/vapor flow, pressure, and temperature control systems are automated to facilitate uninterrupted operation and eliminate daily

Table 1. Summary of experimental input conditions

Experimental design			
Temperature	Pressure	H ₂ :MTS ratio	Total flow ^a
-	+	+	-
+	+	-	+
+	+	+	-
-	+	+	+
-	-	-	+
-	+	-	+
0	0	0	0
0	0	+	0
0	0	--	0
0	+	0	0
+	-	+	+
0	0	0	0
-	-	+	+
+	+	+	+
+	0	0	0
0	0	0	0
+	-	+	-
0	0	-	0
-	-	+	-
0	0	0	+
+	+	-	-
++	0	0	0
+	-	-	-
0	0	0	0
0	-	0	0
0	0	0	-
-	-	-	-
-	+	-	-
-	0	-	-
+	-	-	+

Factor	Factor levels				
	Very low (--)	Low (-)	Median (0)	High (+)	Very high (++)
Temperature (K)	-	1375	1475	1575	1675
Pressure (KPa)	-	10	55	100	-
H ₂ :MTS ratio	5	10	20	35	-
Total flow	-	275	550	1100	-

^aAll flows in cm³/min (STP) at 300 K and 100 KPa.

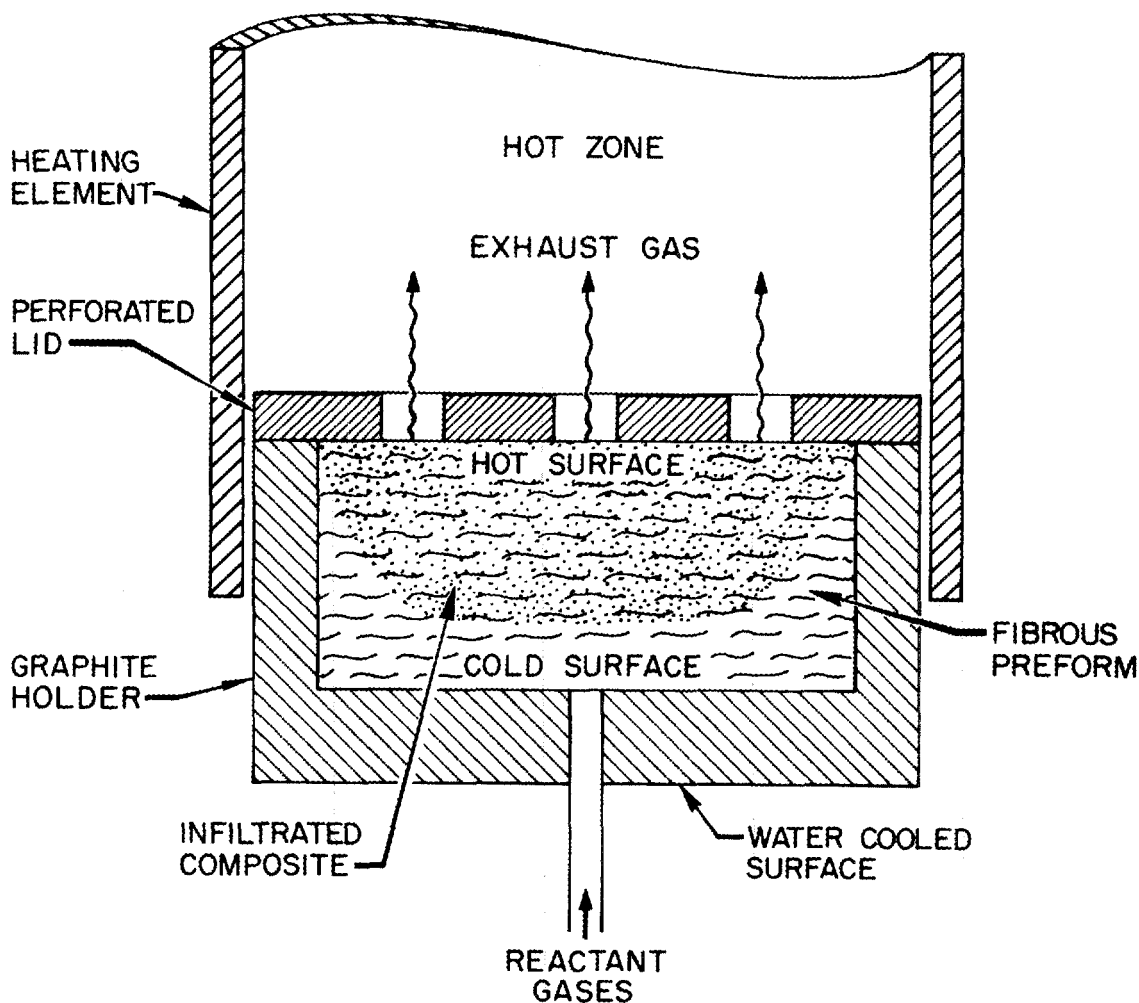


Fig. 1. Schematic of infiltration system.

cycling. Mass flow controllers* were used to set and maintain gas flows and ratios. Methyltrichlorosilane was carried to the reactor by a flow of hydrogen through an evaporator and metered using a vapor source controller.† Pressure control was accomplished using a gas ballast technique, injecting argon gas into the pump inlet to regulate effective

*Type 1259A, MKS Instruments, Inc., 34 Third Ave., Burlington, MA 01803.

†Source V, Tylan, 23301 South Wilmington Ave., Carson, CA 90745.

pumping speed.* The corrected optical temperature at the top surface of the specimen was measured and controlled by a single-wavelength automatic optical pyrometer[†] equipped with a time-proportioning controller. A predetermined pressure differential across the sample designated complete infiltration.

Fibrous preforms were fabricated by stacking multiple layers of plain-weave Nicalon cloth in a 30-60-90° orientation sequence into the cavity of a graphite holder. The layers were compressed and held in place by a perforated graphite lid pinned to the holder. The average fiber content was 41.2 ± 0.8 vol %, 52 layers, with sample dimensions of 45 mm in diameter and 12.5 mm thick. The sizing was then removed from the cloth through multiple washings in acetone. The preform was precoated with a thin layer of pyrolytic carbon to protect the fibers from reactants and products containing chlorine and reduce interfacial bonding to enhance fiber pull-out.²³ The carbon was deposited isothermally by the decomposition of propylene in argon at 1375 K and 5 kPa.²⁷⁻²⁹

The prepared preform had an average theoretical density of 2.91 ± 0.01 g/cm³. The theoretical density is defined as the sum of the products of volume fraction and reported density of each component of the composite (fibers, pyrocarbon, and, after infiltration, SiC). The matrix phase was then deposited from the specified mixtures of H₂ and MTS at the appropriate temperatures and pressures defined by the design.

TESTING

Twelve bend bars [four each from the top, middle, and bottom areas (Fig. 2)] were prepared from each sample to evaluate each one and also to determine variations due to location in the sample. The bars were cut from the samples parallel to the 0-90 orientation of the top layer of cloth using a diamond saw, and tensile and compression surfaces were ground parallel to the long axis of the specimen. The average dimensions of the bars were $2.5 \times 3.3 \times 45$ mm, and all were measured and weighed to

*Type 250B, MKS Instruments, Inc., 34 Third Ave., Burlington, MA 01803.

[†]Modline 2000, Ircon, Inc., 7301 N. Caldwell Ave., Niles, IL 60648.

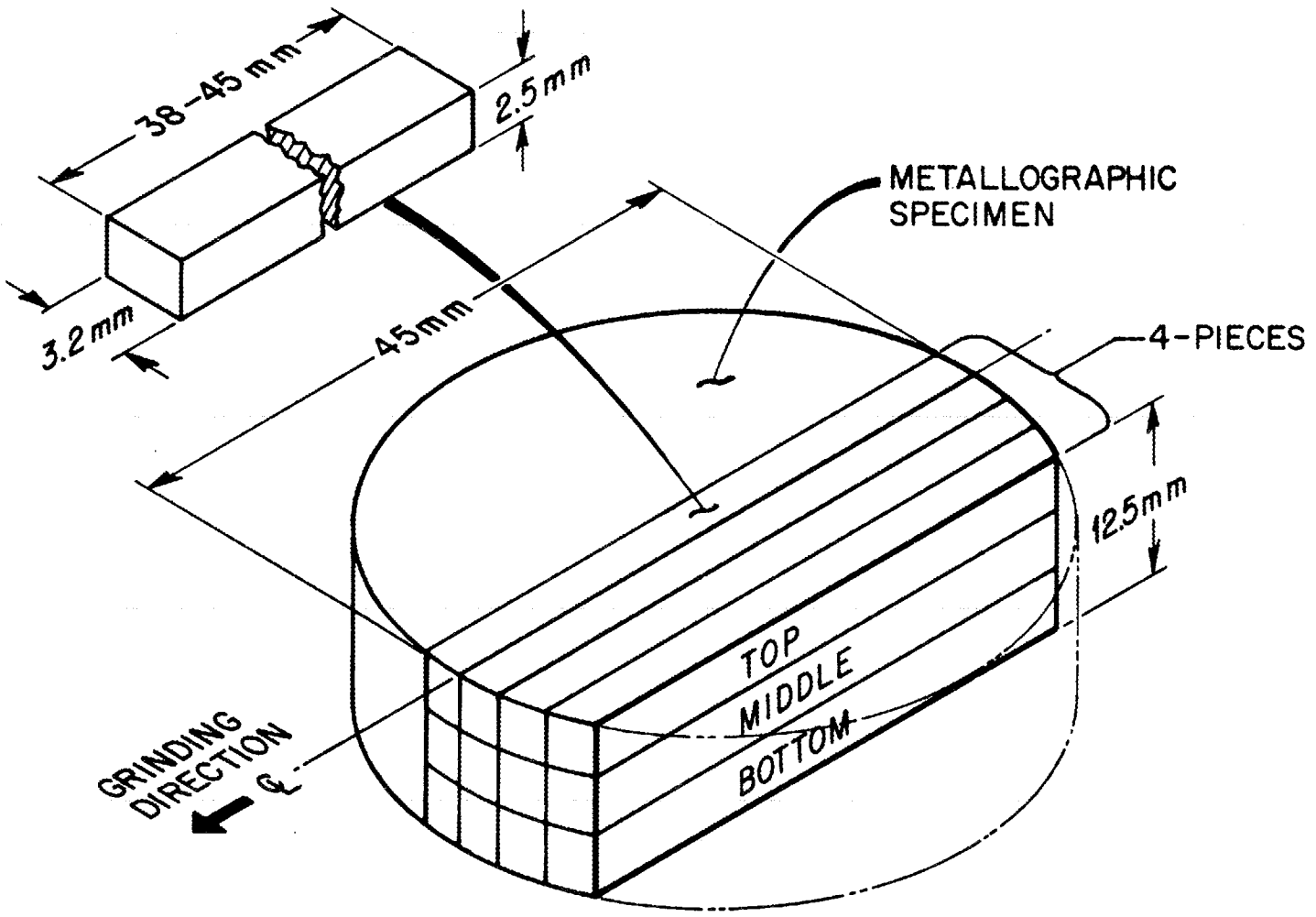


Fig. 2. Location of test specimens within sample.

determine densities. Flexure strengths were measured at room temperature employing four-point bending methods and using a support span of 25.4 mm, a loading span of 6.4 mm, and a crosshead speed of 0.51 cm/min. The load was applied perpendicular to the layers of cloth. Metallographic examination of polished cross sections taken 5 mm off the centerline provided an overall view of the infiltrated sample and coating morphologies.

RESULTS

The results of the experiment are summarized in Tables 2 and 3. Only 28 of the 30 runs were completed. Two runs were deleted when it was recognized that the projected infiltration times were significantly greater than 8 days. A goal of the temperature-gradient forced-flow technique is to decrease processing times.

PROCESSING TIME

The infiltration parameters and resulting completion times for the 28 completed experimental runs are given in Table 2. Three of the four factors considered, temperature, H_2 :MTS ratio, and total gas flow rate, appear to affect infiltration times. Times ranged from 5 h to over 8 days. Examination of the data indicates that time was most effectively reduced by increasing temperature and total gas flow rate, while pressure had little influence. Temperature was the most significant variable, since the majority of the runs processed with a furnace temperature above 1475 K were completed in less than 20 h.

DENSITY

Bulk densities were measured and percentage of theoretical density values were calculated for each of the specimens obtained from the 28 samples. The average values for the top, middle, and bottom layers are reported in Table 3. In some cases, uninfiltreated bottom sections delaminated; thus only 8 of the 12 specimens from a sample were available for examination. In most instances, the highest densities occurred in the top positions, although runs 7 and 10 resulted in radial and axial density

Table 2. Infiltration parameters and resulting processing times

Run	Temperature (K)	Pressure (KPa)	MTS flow ^a	H ₂ flow ^a	H ₂ :MTS ratio	Total flow ^a	Time (h)
1	1375	100	8.0	267	35	275	202.7
2	1575	100	100.0	1000	10	1100	5.3
3	1575	100	8.0	267	35	275	49.0
4	1375	100	31.0	1069	35	1100	50.0
5	1375	10	100.0	1000	10	1100	28.0
6	1375	100	100.0	1000	10	1100	32.0
7	1475	55	26.0	524	20	550	43.6
8	1475	55	15.0	535	35	550	39.3
9	1475	55	92.0	458	5	550	12.0
10	1475	100	26.0	524	20	550	34.4
11	1575	10	31.0	1069	35	1100	12.0
12	1475	55	26.0	524	20	550	24.1
13	1375	10	31.0	1069	35	1100	57.8
14	1575	100	31.0	1069	35	1100	16.8
15	1575	55	26.0	524	20	550	21.5
16	1475	55	26.0	524	20	550	26.8
17	1575	10	8.0	267	35	275	72.0
18	1475	55	50.0	500	10	550	46.4
19	1375	10	8.0	267	35	275	0.0
20	1475	55	52.0	1048	20	1100	12.8
21	1575	100	25.0	250	10	275	18.5
22	1675	55	26.0	524	20	550	7.5
23	1575	10	25.0	250	10	275	17.4
24	1475	55	26.0	524	20	550	26.1
25	1475	10	26.0	524	20	550	63.5
26	1475	55	13.0	262	20	275	53.1
27	1375	10	25.0	250	10	275	0.0
28	1375	100	25.0	250	10	275	51.3
29	1375	55	26.0	250	10	275	112.5
30	1575	10	100.0	1000	10	1100	14.1

^aAll flows in cm³/min (STP) at 300 K and 100 KPa.

Table 3. Density and flexure strength results^a

Run	Position	Density (g/cm ³)	Std. dev.	%T.D. ^b	Strength (MPa)	Std. dev.	Run	Position	Density (g/cm ³)	Std. dev.	%T.D. ^b	Strength (MPa)	Std. dev.
1	Top	2.53	0.01	86.8	301	32	15	Top	2.48	0.03	85.5	318	30
1	Middle	2.48	0.01	85.2	294	13	15	Middle	2.51	0.02	86.5	320	18
1	Bottom	2.28	0.03	78.5	247	5	15	Bottom	2.01	0.03	69.3	120	34
2	Top	2.42	0.01	82.8	265	21	16	Top	2.51	0.01	86.5	351	25
2	Middle	2.32	0.02	79.6	248	15	16	Middle	2.43	0.09	83.9	447	20
3	Top	2.33	0.03	80.0	334	30	16	Bottom	1.84	0.02	63.4	158	23
3	Middle	2.14	0.03	73.6	286	18	17	Top	2.44	0.02	83.5	236	25
3	Bottom	2.21	0.03	75.9	263	46	17	Middle	2.34	0.03	80.1	252	9
4	Top	2.48	0.02	85.5	299	13	17	Bottom	1.80	0.08	61.6	145	49
4	Middle	2.34	0.01	80.8	278	14	18	Top	2.61	0.01	89.9	344	46
5	Top	2.47	0.02	85.1	394	18	18	Middle	2.22	0.02	76.6	216	3
5	Middle	2.29	0.01	78.8	306	8	18	Bottom	1.87	0.02	64.4	104	10
5	Bottom	2.03	0.02	70.1	156	10	20	Top	2.53	0.01	86.9	450	12
6	Top	2.55	0.02	87.3	359	44	20	Middle	2.43	0.01	83.5	403	25
6	Middle	2.44	0.01	83.3	268	9	20	Bottom	2.11	0.04	72.8	311	13
7	Top	2.52	0.01	86.5	313	11	21	Top	2.52	0.01	87.2	417	18
7	Middle	2.50	0.02	85.9	346	22	21	Middle	2.47	0.02	85.5	406	30
7	Bottom	2.50	0.02	85.8	385	43	21	Bottom	2.44	0.02	84.4	390	14
8	Top	2.35	0.02	80.9	277	19	22	Top	2.32	0.01	79.5	321	22
8	Middle	2.44	0.04	84.3	311	22	22	Middle	2.35	0.01	80.8	353	10
8	Bottom	2.57	0.02	88.6	371	13	22	Bottom	2.27	0.03	77.8	350	24
9	Top	2.53	0.02	87.2	436	4	23	Top	2.58	0.03	88.2	396	30
9	Middle	2.45	0.01	84.4	354	11	23	Middle	2.57	0.01	87.8	354	44
9	Bottom	2.28	0.01	78.6	311	14	23	Bottom	2.49	0.03	85.4	308	26
10	Top	2.49	0.01	85.6	325	18	24	Top	2.59	0.01	88.8	471	3
10	Middle	2.51	0.02	86.0	349	14	24	Middle	2.54	0.01	87.1	410	22
10	Bottom	2.49	0.02	85.4	343	30	24	Bottom	2.33	0.01	80.1	344	7
11	Top	2.29	0.03	78.7	260	14	25	Top	2.43	0.02	84.1	333	13
11	Middle	2.46	0.02	84.8	345	14	25	Middle	2.24	0.02	77.7	274	10
11	Bottom	2.42	0.02	83.4	348	50	26	Top	2.53	0.02	86.9	274	25
12	Top	2.54	0.02	87.4	324	18	26	Middle	2.42	0.04	83.1	272	38
12	Middle	2.51	0.01	86.5	410	34	26	Bottom	2.06	0.06	70.8	142	10
12	Bottom	2.30	0.02	79.2	303	6	28	Top	2.62	0.02	90.1	430	10
13	Top	2.49	0.01	86.4	450	16	28	Middle	2.56	0.01	88.0	421	28
13	Middle	2.35	0.05	81.4	405	24	28	Bottom	2.40	0.06	82.7	478	34
14	Top	2.41	0.02	83.0	283	27	29	Top	2.64	0.01	90.9	447	46
14	Middle	2.48	0.03	85.3	357	28	29	Middle	2.63	0.01	90.6	440	23
14	Bottom	2.05	0.03	70.6	162	13	29	Bottom	2.56	0.01	88.2	422	18
							30	Top	2.48	0.03	85.0	343	13
							30	Middle	2.52	0.02	86.5	337	14
							30	Bottom	2.27	0.09	78.0	228	19

^aAverage of four values for each layer.^bDensity of SiC = 3.21 g/cm³, Pyc = 2.00 g/cm³, and Nicalon = 2.55 g/cm³.

gradients of <1% for an average density of 2.50 g/cm³. Values as high as 2.65 g/cm³, 91.2% of theoretical density, were measured, but the density frequently decreased toward the bottom (cooled side) of the preform. A typical polished cross section of a completed composite sample is shown in Fig. 3.

ROOM-TEMPERATURE FLEXURE STRENGTH

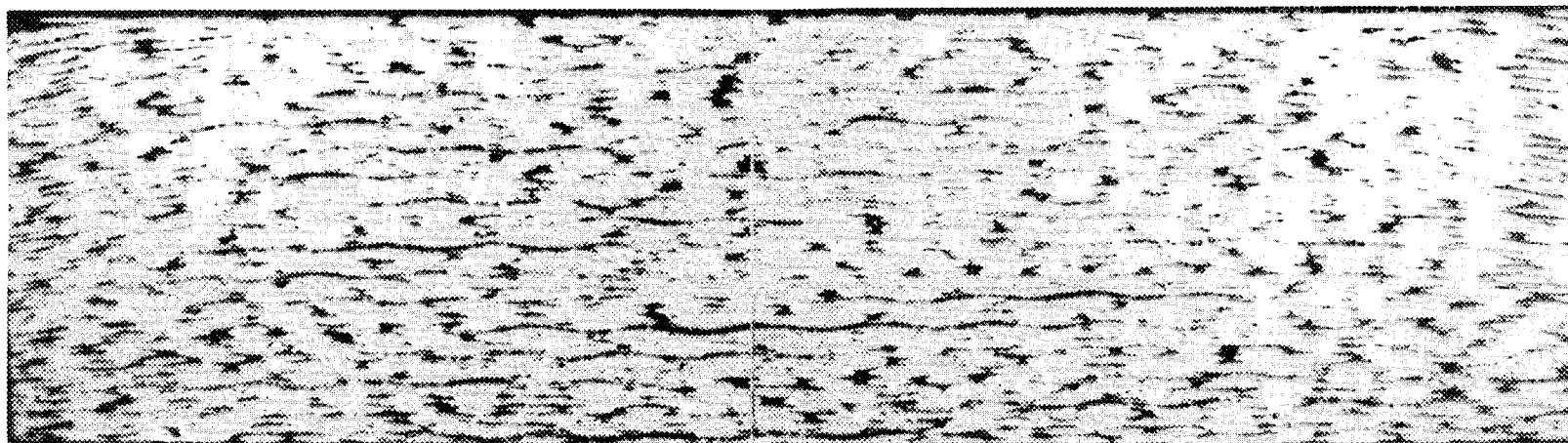
Flexure strengths of the composite specimens were measured by four-point bending and ranged from 83 to 517 MPa. All specimens exhibited composite behavior during testing, as demonstrated by fiber pull-out and by the appearance of the load-crosshead displacement curves (Fig. 4). The results are reported in Table 3 as the average values across each layer. Examination of the data reveals a modest positive correlation between density and strength. A plot of these two values for all specimens tested is shown in Fig. 5. The correlation coefficient is 0.764, and the corresponding p value is <0.0001. Although buckling at the compressive surface and cracking parallel to the tensile surface occur during testing and thus failure occurs not in simple tension but by a complex combination of tension, compression, and shear, flexure strengths are adequate to obtain a relative measure of the strength of the composites fabricated under different infiltration conditions.

PROCESS RELATIONSHIPS

The experiments were designed to evaluate the effects of controlled input variables on the infiltration process. In order to predict given responses across a range of variables, each point must be itself reproducible. Reproducibility within the experimental design was verified by repeating the central point four times. These are run numbers 7, 12, 16, and 24 in the sequence (Table 3). Neglecting the bottom locations, examination of the standard deviations of density and strength within these four show that the variability within the group was <2% for density and <15% for strength, making it possible to relate them to the response variables, time, density achieved, and strength, as a function of the input parameters, temperature, pressure, H₂:MTS ratio, and total gas flow.

ORNL-PHOTO 3153-87

HOT FACE



COLD FACE

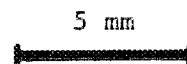


Fig. 3. Cross section of an infiltrated sample.

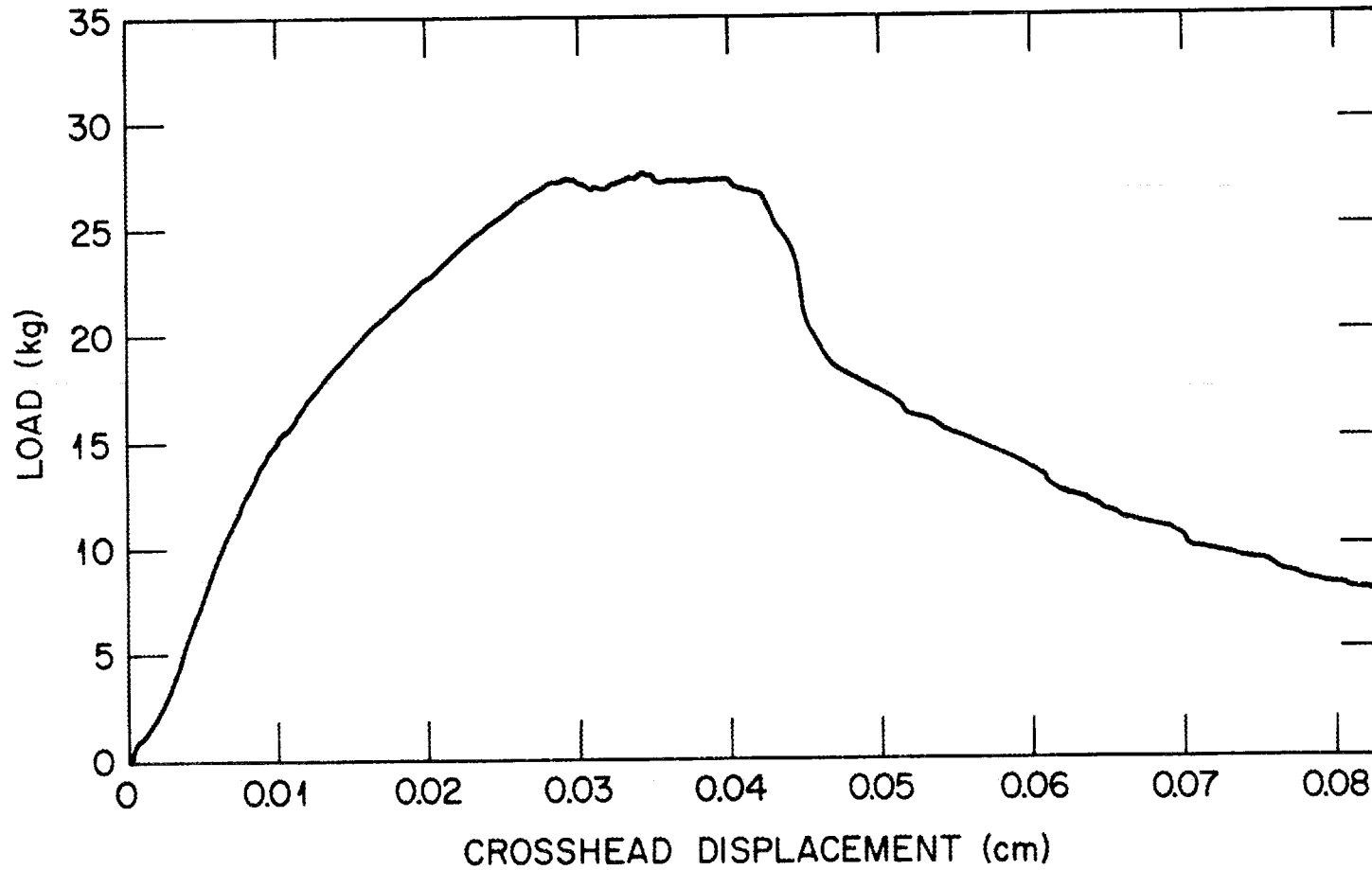


Fig. 4. Curve of load vs crosshead displacement for SiC/Nicalon composite tested in 4-point flexure at room temperature.

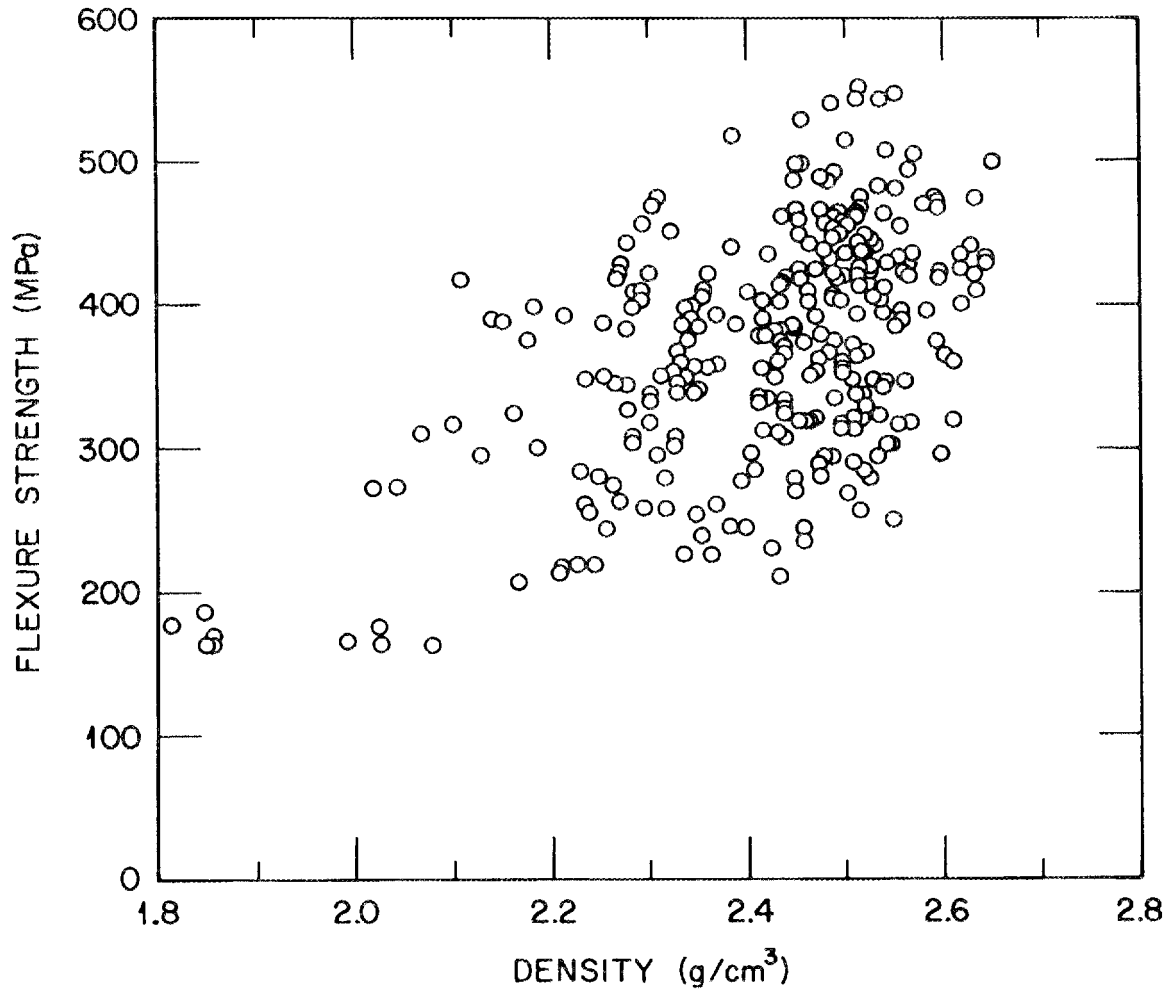


Fig. 5. Plot of room-temperature flexure strength vs density for all specimens tested.

Using multiple linear regression, an equation relating infiltration time and the process parameters was derived and shown to be statistically significant but lacked precision, with an R^2 of 59%. The precision of the relationship was considerably improved by utilizing the natural logarithm of time, resulting in an R^2 of 82%. The final form of the time equation is:

$$\begin{aligned} \ln [\text{time (h)}] = & 12 (\pm 1) - 6.8 (\pm 0.8) \times 10^{-3} [T (\text{K})] \\ & - 4.3 (\pm 3.6) \times 10^{-5} [P (\text{kPa})] \\ & + 3.3 (\pm 0.7) \times 10^{-2} [\text{vol ratio (H}_2\text{:MTS)}] \\ & - 1.4 (\pm 0.2) \times 10^{-3} [\text{flow rate (cm}^3\text{/min)}]. \end{aligned}$$

The gradient of this fitted surface at the central point indicates that infiltration time is decreased not only by increased temperature and total flow rate but also by reduced H₂:MTS ratios. The shortest time, 5.3 h, resulted from a furnace temperature of 1575 K, a pressure of 100 kPa, a total flow of 1100 cm³/min, and an H₂:MTS ratio of 10:1. The conditions for the longest, 202.7 h, were 1375 K, 100 kPa, a total flow rate of 275 cm³/min, and an H₂:MTS ratio of 35:1.

Statistical analysis of the densities as a function of the experimental variables indicated that the only values that could be related with any accuracy were the top-row averages. The bottom layers were unpredictable for many sets of conditions, leading to an R² of <30%. In addition, first-order linear regression did not fit well, and thus mixed quadratic terms were added to account for the interactions of the four process parameters. The equation for top-row average density thus derived has an R² of 82% and is given in Table 4. Evaluation of the gradient of the equation at the central point suggests that density is most effectively

Table 4. Relationship for top row average density

Parameter	Estimate
Intercept	118 (±18) %
a	-0.02 (±0.01) % / K
b	0.16 (0.16) % / KPa
c	1.02 (0.61) %
d	-0.03 (0.02) % /cm ³ /min
e	1.15 (1.30) × 10 ⁻⁴ % / K KPa
f	-7.37 (3.47) × 10 ⁻³ % / K
g	2.14 (1.45) × 10 ⁻⁵ %/K cm ³ /min
h	-8.50 (10.2) × 10 ⁻⁴ % / KPa
i	6.40 (3.18) × 10 ⁻⁵ % / KPa cm ³ /min
j	5.92 (1.11) × 10 ⁻⁵ % / cm ³ /min

$$\begin{aligned} \text{T.D. (\%)} = & 118 + (a \times T) + (b \times P) + (c \times R) + (d \times F) + (e \times T \times P) \\ & + (f \times T \times R) + (g \times T \times F) + (h \times P \times R) + (i \times P \times F) \\ & + (j \times R \times F) \end{aligned}$$

T = temperature (K),
P = pressure (KPa),
R = molar ratio of H₂/MTS,
F = total gas flow (cm³/min).

increased by reducing temperature, H₂:MTS ratio, and total flow rate. Again, pressure had little influence. This trend is supported by the facts that runs 28 and 29 produced the highest top-row densities and that both of these had temperature, H₂:MTS ratio, and total gas flow rate at their respective lowest values.

The same fitting procedure used to relate density was also used to correlate flexural strength with the four process parameters. As with density measurements, the bottom areas yielded the greatest variations and were deleted during analysis. The relationship for top-row average strength has an R of 83% but contains high standard errors for individual estimates due to a combination of possible redundancies in the equation and the exclusion of undetermined factors.

DISCUSSION

THERMODYNAMICS AND KINETICS

The chemical vapor deposition of SiC from MTS is a relatively simple process and has been extensively examined.³⁰⁻³⁴ Methyltrichlorosilane contains silicon and carbon in stoichiometric proportions and is a liquid with a reasonable vapor pressure, making it a good reactant for vapor deposition. Thermodynamic analyses of the Si-C-H-Cl system (using SOLGASMIX-PV³⁵⁻³⁷) have been previously reported,^{37,38} but an analysis was made in this study to include conditions bounded by the experimental design. The thermodynamic analysis was conducted using the EQUILIB computer program of the F*A*C*T system.* The equilibria were defined by specifying temperature, pressure, and the molar ratio of H₂:MTS. Three condensed phases (Si, α-SiC, and β-SiC) and 81 gas species were considered. Previous investigators have shown that the formation of carbon is kinetically hindered under the conditions considered; thus it was omitted in this analysis.^{37,39} The results of the thermodynamic calculations were used to calculate theoretical deposition efficiencies by dividing the equilibrium yields by the yield as determined from the molar quantity of MTS (Figs. 6 and 7).

*EQUILIB, F*A*C*T, W. T. Thompson, Royal Military College of Canada, and A. D. Pelton and C. W. Bale, Ecole Polytechnique, Montreal.

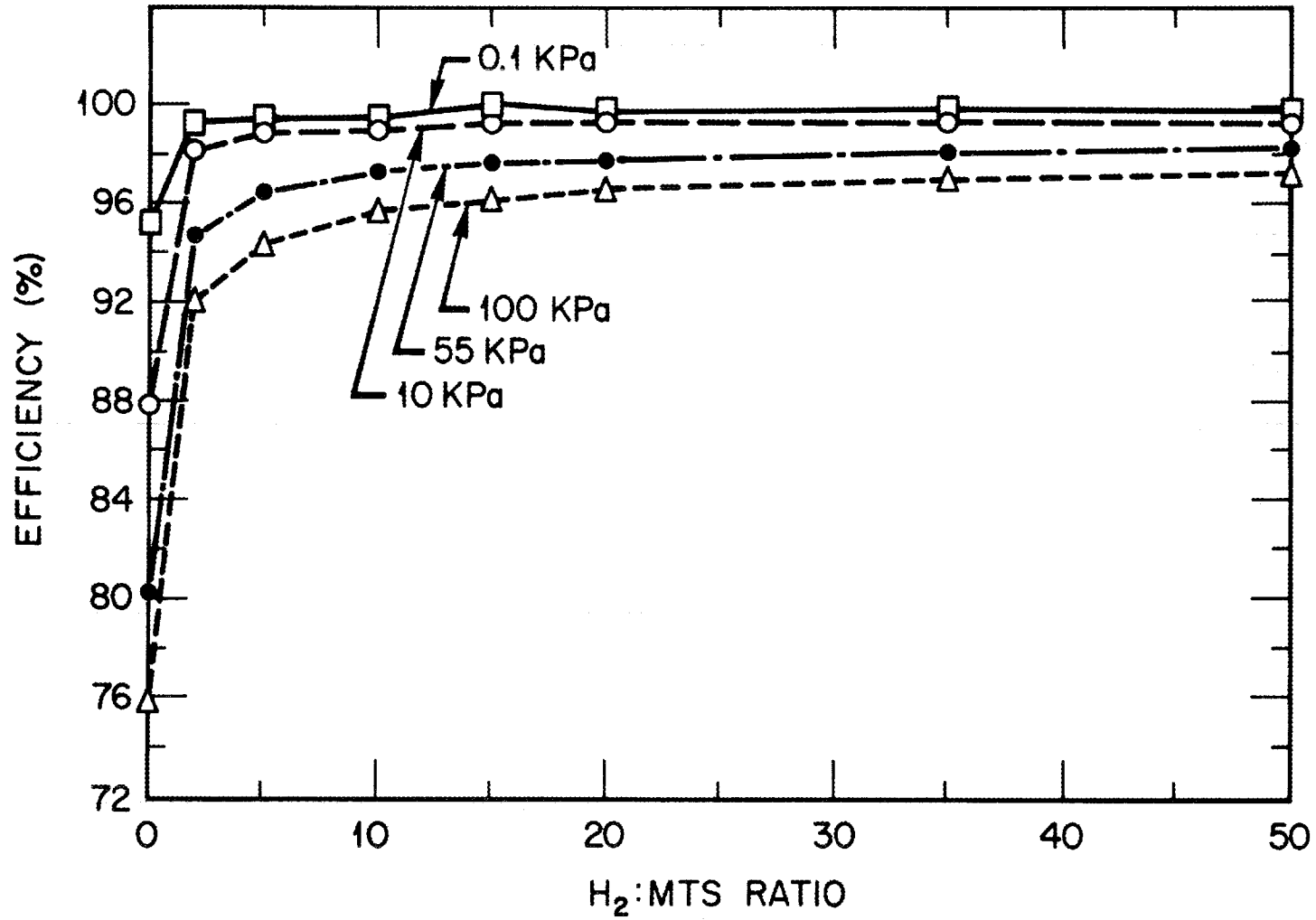


Fig. 6. Calculated deposition efficiencies as a function of H₂:MTS ratio and pressure.

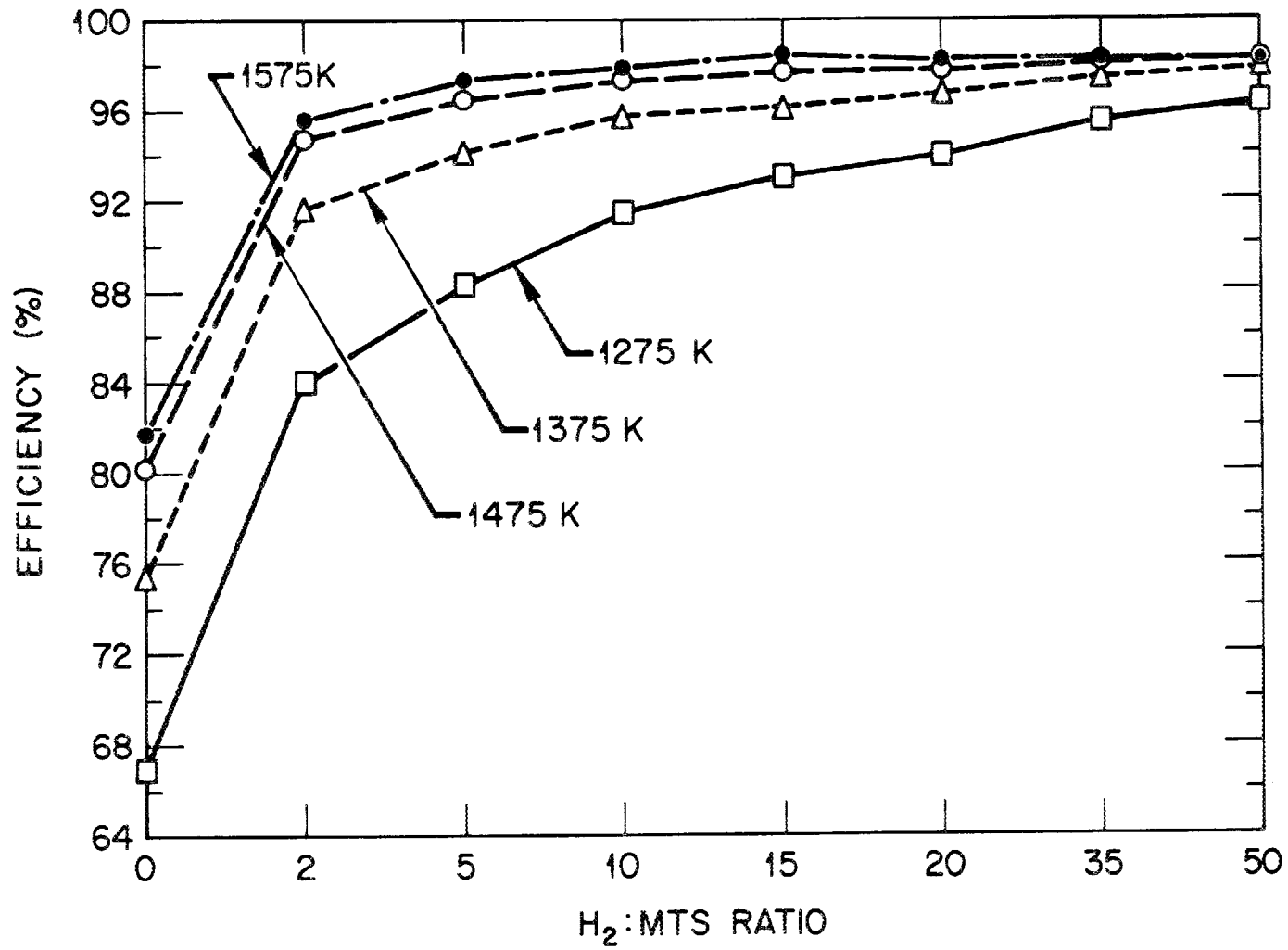


Fig. 7. Calculated deposition efficiencies as a function of H₂:MTS ratio and temperature.

PRESSURE

Pressure appeared to have little or no effect on the response variables. It was originally assumed that reducing the processing pressure would decrease deposition rates and, therefore, increase infiltration times due to increased gas velocities and decreased residence times.⁴⁰ At the reduced pressures considered (55 and 10 kPa), the linear gas velocities are 1.8 and 12.7 times higher, respectively, than at local atmospheric pressure. This implies greatly reduced residence times of the gases within the preform. At the central-point total gas flow rate of 550 cm³/min, the residence time is 3.7×10^{-2} , while the residence times for the reduced pressures are calculated to be 2.0×10^{-2} and 2.9×10^{-3} s, respectively. Thus, these factors should decrease coating rates, but this was not observed.

Different mechanisms associated with reduced pressure may affect deposition efficiency. Figure 6 displays the equilibrium deposition efficiency of SiC as a function of H₂:MTS ratios at various pressures as predicted by thermodynamic calculation. The graph indicates an increase in deposition efficiency with reduced pressure. An isothermal decrease in pressure shifts equilibrium toward the products SiC and HCl. These combined with higher diffusion rates, also associated with reduced pressure, could counteract the effects of increased gas velocities.

TEMPERATURE

A plot of predicted deposition rates with respect to gas composition at the different furnace temperatures used in the statistical study is shown in Fig. 7. Increasing the furnace temperature increases the deposition efficiency, and this is reflected in the observed reduction of infiltration times at higher temperatures. The average flexure strengths of the samples processed at 1575 K were lower than those of samples infiltrated at 1375 and 1475 K. A reduction of strength in the final material is expected, since Nicalon fibers degrade at elevated temperatures.^{41,42}

An increase in achieved density was noted in the respective low-temperature runs. The decrease in deposition rates at this condition may allow open porosity in the upper areas to remain for a longer fraction of

the run time. Reactant gases are thus able to permeate a larger percentage of the volume, resulting in more complete and uniform infiltration.³⁹

TOTAL FLOW RATE

In general, the total gas flow had the same contributive effect as temperature. Time was decreased as the flows were increased, and higher densities were attained at lower gas flow rates. Early studies of SiC coatings from chlorosilanes determined that the rate-controlling factor was the reactant supply rate.³¹ High deposition rates occur at high levels of flow and low ratios of hydrogen to methyltrichlorosilane.

A detrimental effect of high gas flows in the temperature-gradient pressure-gradient process was the lack of deposition in the bottom layers. The increased flow rate of gas cools the lower surface and disturbs the temperature gradient. This is enhanced by the basic principles and designs present in the gas injection and distribution systems, which cause the reactant gases and graphite holder to be cooled at the same rate regardless of deposition conditions.

HYDROGEN:MTS RATIO

In Figs. 6 and 7 it is evident that increasing the ratio of hydrogen to MTS has a positive effect on the deposition efficiency up to a ratio of 12:1, where leveling occurs. In the series of experimental runs, a decrease in the ratio resulted in a favorable response with respect to all three output variables. A decrease in H₂:MTS ratio corresponds to an increase in reactant concentration; thus, lowering the H₂:MTS ratio also decreased the likelihood of codepositing silicon. Codeposition occurs when the ratio of hydrogen to silicon in the Si-C-H-Cl gas mixture is high or the reaction is carried out at low temperature.³⁸ Several investigations have determined that deposition of single-phase SiC occurs at H₂:Si = 5 or less at a temperature of 1473 K, Si:C = 1, and Cl:Si = 3 (ref. 37). Higher-quality material is therefore produced at the lower ratios.

CONCLUSIONS

The thermal-gradient pressure-gradient process for the fabrication of ceramic-fiber-reinforced ceramic-matrix composites was studied in response to the following experimental variables: temperature, pressure, total gas flow, and H₂:MTS ratio. These parameters influenced achieved density, flexure strength, and infiltration time. The information obtained has advanced the progress toward developing an efficient method for producing high density and high strength composites.

Runs 7 and 10 produced samples with density variations throughout of less than 1% of the average 86.1% and 85.6% of theoretical, confirming that uniform infiltration is attainable. The statistical analysis indicated that within the boundaries of the experiment, a temperature of 1473 K, an H₂:MTS ratio of less than 10:1, and a total gas flow of 550 cm³/min would result in high strength, density, and uniformity in a comparatively short processing time. The operating pressure was found to be statistically insignificant; thus infiltration at atmospheric pressure simplifies processing. Combining these results and trends, material with uniform physical properties can be produced.

Multiple linear regression techniques were employed to relate the response of the process and the properties of the fabricated composite material to the experimental variables. The relationships of infiltration time, density, and room-temperature flexure strength to the input parameters of temperature, pressure, H₂:MTS ratio, and total gas flow were determined. Relatively accurate responses can be calculated from the predictive equations.

ACKNOWLEDGMENTS

The authors recognize R. A. Lansberry for assistance in physical property measurements. Appreciation is due: E. L. Long, Jr. and M. A. Janney for manuscript review, B. Q. Atkinson for preparation for publication, and C. A. Valentine for typing the draft.

REFERENCES

1. J. Aveston and A. Kelly, "Theory of Multiple Fracture of Fibrous Composites," *J. Mater. Sci.* **8**, 352-62 (1973).
2. D. B. Marshal and A. G. Evans, "Failure Mechanisms in Ceramic-Fiber/Ceramic Matrix Composites," *J. Am. Ceram. Soc.* **68**, 225-31 (1985).
3. R. W. Rice, "Mechanisms of Toughening in Ceramic Matrix Composites," *Ceram. Eng. Sci. Proc.* **2**(7-8), 661-701 (1981).
4. K. M. Prewo and J. J. Brennan, "High-Strength Silicon Carbide Fiber-Reinforced Glass-Matrix," *J. Mater. Sci.* **15**, 463-68 (1980).
5. K. M. Prewo and J. J. Brennan, "Silicon Carbide Yarn Reinforced Glass Matrix Composites," *J. Mater. Sci.* **17**, 1201-6 (1982).
6. J. J. Brennan and K. M. Prewo, "Silicon Carbide Fiber-Reinforced Glass-Matrix Composites Exhibiting High Strength and Toughness," *J. Mater. Sci.* **17**, 2371-82 (1982).
7. W. A. Bryant, "The Fundamentals of Chemical Vapour Deposition," *J. Mater. Sci.* **12**, 1285-1306 (1977).
8. W. H. Pfiefer et al., "Consolidation of Composite Structures by CVD," pp. 463-85 in *Second Int. Conf. Chem. Vapor Dep.*, ed. J. M. Blocher, Jr., and J. C. Whithers, Electrochemical Society, New York, 1970.
9. H. O. Pierson and J. F. Smatana, "Carbon Composites from Wool Substrates," pp. 487-505 in *Second Int. Conf. Chem. Vapor Dep.*, ed. J. M. Blocher, Jr., and J. C. Whithers, Electrochemical Society, New York, 1970.
10. J. C. Whithers, "Chemical Vapor Deposition of Ceramic Composites Containing Whisker and Fiber Reinforcements," pp. 507-19 in *Second Int. Conf. Chem. Vapor Dep.*, ed. J. M. Blocher, Jr., and J. C. Whithers, Electrochemical Society, New York, 1970.
11. L. R. Newkirk et al., "Chemical Vapor Deposition Fabrication of Filament Reinforced Composites for High Temperature Applications," pp. 82-101 in *Chemically Vapor Deposited Coatings*, ed. H. O. Pierson, American Ceramic Society, Columbus, Ohio, 1981.

12. J. J. Gebhart, "CVD Boron Nitride Infiltration of Fibrous Structures: Properties of Low Temperature Deposits," pp. 469-72 in *Fourth Int. Conf. Chem. Vapor Dep.*, ed. G. F. Wakefield and J. M. Blocher, Jr., Electrochemical Society, Princeton, N.J., 1973.
13. F. Christin, R. Naslain, and C. Bernard, "A Thermodynamic and Experimental Approach of Silicon Carbide-CVD Application to the CVD-Infiltration of Porous Carbon-Carbon Composites," pp. 499-514 in *Proc. Seventh Int. Conf. Chem. Vapor Dep.*, ed. G. F. Wakefield and J. M. Blocher, Jr., Electrochemical Society, Princeton, N.J., 1973.
14. R. Naslain, H. Hannache, L. Heraud, J. Rossignol, F. Christin, and C. Bernard, "Chemical Vapor Infiltration Techniques," pp. 293-304 in *Euro-CVD-Four*, Eindhoven, Netherlands, 1983.
15. H. Hannache, R. Naslain, and C. Bernard, "Boron Nitride Chemical Vapour Infiltration of Fibrous Materials from $\text{BCl}_3\text{-NH}_3\text{H}_2$ or $\text{BF}_3\text{-NA}_3$ Mixtures: A Thermodynamic and Experimental Approach," *J. Less-Common Met.* **95**, 221-46 (1983).
16. J. Rossignol, I. Langlais, and R. Naslain, "A Tentative Modelization of Titanium Carbide CVI Within the Pore Network of Two-Dimensional Carbon-Carbon Composite Preforms," pp. 596-614 in *Ninth Int. Conf. Chem. Vapor Dep.*, ed. M. Robinson, G. Cullen, C. Van den Brekel, and J. M. Blocker, Jr., Electrochemical Society, Princeton, N.J., 1984.
17. A. J. Caputo and W. J. Lackey, "Process for the Preparation of Fiber-Reinforced Ceramic Composites by Chemical Vapor Deposition", U.S. patent 4,580,523, April 8, 1986.
18. A. J. Caputo and W. J. Lackey, *Fabrication of Fiber-Reinforced Ceramic Composites by Chemical Vapor Infiltration*, ORNL/TM-9235, October 1984.
19. A. J. Caputo and W. J. Lackey, "Fabrication of Fiber-Reinforced Ceramic Composites by Chemical Vapor Infiltration," *Ceram. Eng. Sci. Proc.* **5**(7-8), 654-67 (1984).
20. A. J. Caputo, W. J. Lackey, and D. P. Stinton, "Development of a New, Faster Process for the Fabrication of Ceramic Fiber-Reinforced Ceramic Composites by Chemical Vapor Infiltration," *Ceram. Eng. Sci. Proc.* **6**(7-8), 694-706 (1985).

21. A. J. Caputo, R. A. Lowden, and D. P. Stinton, *Improvements in the Fabrication of Ceramic-Fiber-Ceramic-Matrix Composites by Chemical Vapor Deposition*, ORNL/TM-9651, June 1985.
22. D. P. Stinton, A. J. Caputo, and R. A. Lowden, "Synthesis of Fiber-Reinforced SiC Composites by Chemical Vapor Infiltration," *Am. Ceram. Soc. Bull.* 65(2), 347-50 (1986).
23. A. J. Caputo, R. A. Lowden, and D. P. Stinton, "Fiber-Reinforced SiC Composites With Improved Mechanical Properties," *Am. Ceram. Soc. Bull.* 66(2), 368-72 (1987).
24. G. E. P. Box, W. G. Hunter, and J. S. Hunter, *Statistics for Experimenters*, Wiley, New York, 1978.
25. W. G. Cochran and G. M. Cox, *Experimental Designs*, Wiley, New York, 1950.
26. R. H. Myers, *Response Surface Methodology*, Allyn and Bacon, Inc., Boston, 1971.
27. W. V. Kotlensky, "Deposition of Pyrolytic Carbon in Porous Solids," *Chem. Phys. Carbon* 9, 173-262 (1973).
28. B. Dacic and S. Marikovic, "Carbon Fiber/Carbon Composites by CVD from Propylene," pp. 616-63 in *Carbon '80 (Int. Carbon Conf., 3rd)*, 1980.
29. H. O. Pierson and M. L. Lieberman, "The Chemical Vapor Deposition of Carbon on Carbon Fibers," *Carbon* 13, 159-66 (1975).
30. T. D. Gulden, "Deposition and Microstructure of Vapor Deposited Silicon Carbide," *J. Am. Ceram. Soc.* 51(8), 424-27 (1968).
31. T. D. Gulden, "Mechanical Properties of Polycrystalline BetaSiC," *J. Am. Ceram. Soc.* 52(11), 585-90 (1969).
32. R. J. Price, "Structure and Properties of Pyrolytic Silicon Carbide," *Am. Ceram. Soc. Bull.* 48(9), 859-62 (1969).
33. D. P. Stinton and W. J. Lackey, "Effect of Deposition Conditions on the Properties of Pyrolytic SiC Coatings for HTGR Fuel Particles," *Am. Ceram. Soc. Bull.* 47(6), 568-73 (1978).
34. J. I. Federer, *Fluidized Bed Deposition and Evaluation of Silicon Carbide Coatings on Microspheres*, ORNL/TM-5152, January 1977.
35. G. Eriksson, "Thermodynamic Studies of High-Temperature Equilibria," *Chem. Scr.* 8(3), 100-03 (1975).

36. T. M. Besmann, *SOLGASMIX-PV, A Computer Program to Calculate Equilibrium Relationships in Complex Chemical Systems*, ORNL/TM-5775, April 1977.
37. J. Chin, P. K. Ganzel, and R. G. Hudson, "The Structure of Chemical Vapor Deposited Silicon Carbide," *Thin Solid Films* **40**, 57-72 (1977).
38. G. S. Fischman and W. T. Petuskey, "Thermodynamic Analysis and Kinetic Implications of Chemical Vapor Deposition of SiC from Si-C-Cl-H Gas Systems," *J. Am. Ceram. Soc.* **68**(4), 185-90 (1985).
39. P. Krautwasser, G. M. Begun, and P. Angelini, "Raman Spectral Characterization of Silicon Carbide Nuclear Fuel Coatings," *J. Am. Ceram. Soc.* **66**(6), 424-34 (1983).
40. E. Fitzner and R. Gadow, "Fiber-Reinforced Silicon Carbide," *Am. Ceram. Soc. Bull.* **65**(2), 326-35 (1986).
41. T. Mah et al., "Thermal Stability of SiC Fibers," *J. Mater. Sci.* **19**, 1191-1201 (1984).
42. H. H. Moeller and J. H. Worley, "Tensile Testing of Ceramic Fiber Tows," *Ceram. Eng. Sci. Proc.* **6**(7-8), 558-66 (1985).

INTERNAL DISTRIBUTION

- | | | | |
|--------|-------------------------------|--------|-----------------------------|
| 1-2. | Central Research Library | 25-29. | R. A. Lowden |
| 3. | Document Reference Section | 30. | R. W. McClung |
| 4-5. | Laboratory Records Department | 31. | R. E. Pawel |
| 6. | Laboratory Records, ORNL RC | 32. | A. C. Schaffhauser |
| 7. | ORNL Patent Section | 33. | M. A. Schmidt |
| 8. | P. Angelini | 34-38. | D. P. Stinton |
| 9. | R. L. Beatty | 39-41. | P. T. Thornton |
| 10-14. | T. M. Besmann | 42. | J. R. Weir |
| 15. | R. A. Bradley | 43. | G. Y. Chin (Consultant) |
| 16-20. | A. J. Caputo | 44. | H. E. Cook (Consultant) |
| 21. | R. H. Cooper | 45. | F. F. Lange (Consultant) |
| 22. | D. R. Johnson | 46. | T. E. Mitchell (Consultant) |
| 23. | R. R. Judkins | 47. | W. D. Nix (Consultant) |
| 24. | E. L. Long, Jr. | 48. | J. C. Williams (Consultant) |

EXTERNAL DISTRIBUTION

49. ACUREX CORPORATION, 555 Clyde Avenue, P. O. Box 7555,
Mountain View, CA 94039
R. Chang
50. ADIABATICS, INCORPORATED, 630 S. Mapleton, Columbus, IN 47201
Roy Kamo, President
- 51-52. AFWAL/MLLM, Wright-Patterson AFB, OH 45433
Henry Graham
Alan Katz
- 53-56. AIR PRODUCTS AND CHEMICALS, INC., P.O. Box 538T, Allentown, PA 18105
P. N. Dyer R. K. Malhotra
V. L. Magnotta S. V. Raman
57. AIRCO TEMESCAL, 2850 Seventh Street at Heinz, Berkeley, CA 94710
Ernest Demiray
58. AIRESEARCH MANUFACTURING COMPANY, 2525-T West 190th Street,
Torrance, CA 90509
D. M. Kotchick
59. ARCO CHEMICALS COMPANY, Silag Operation, Route 6, Box A,
Greer, SC 29651
J. F. Rhodes

60. ARGONNE NATIONAL LABORATORY, 9700 South Cass Avenue, Argonne, IL
60439
W. A. Ellingson
- 61-62. ARMY MATERIALS AND MECHANICS RESEARCH CENTER, Arsenal Street,
Watertown, MA 02172
R. N. Katz
J. W. McCauley
63. AVCO, 201 Lowell Street, Wilmington, MA 01887
Tom Vasilos
- 64-65. AVCO SPECIALTY MATERIALS, 2 Industrial Avenue, Lowell, MA 01851
B. Belason
T. F. Foltz
- 66-69. BABCOCK & WILCOX COMPANY, Lynchburg Research Center, P.O. Box 239,
Lynchburg, VA 24505
L. J. Ferrell
W. G. Long
H. H. Moeller
D. R. Petrak
- 70-71. BATTELLE COLUMBUS LABORATORIES, 505 King Avenue, Columbus, OH
43201
S. P. Mukherjee
I. G. Wright
- 72-75. BATTELLE PACIFIC NORTHWEST LABORATORIES, P.O. Box 999,
Battelle Boulevard, Richland, WA 99352
Ed Cartwright
T. D. Chikalla
S. D. Dahlgren
Ed. McClanahan
76. CABOT CORPORATION, 125 High Street, Boston, MA 02110
Nicholas Fiore
- 77-79. CATERPILLAR TRACTOR COMPANY, Peoria, IL 61629
M. B. Beardsky
M. Haselkorn
G. G. Volbert
80. CERAMATEC, INC., 163 West 1700 Street, Salt Lake City, UT 84115
D. W. Richerson

- 81-84. CORNING GLASS WORKS, Corning, NY 14831
K. Chyung D. C. Larson
R. C. Doman P. Papa
- 85-87. CUMMINS ENGINE COMPANY, INC., 1000 5th St., Columbus, IN 47201
J. W. Patten
G. L. Starr
T. M. Yonushonis
88. DOW CORNING CORPORATION, 3901 South Saginaw Road, Midland, MI
48640
H. W. Foglesong
- 89-90. FORD MOTOR COMPANY, Engineering and Research, P.O. Box 2053,
Dearborn, MI 48121
D. L. Hartsock
A. F. McLean
- 91-92. GA TECHNOLOGIES, P.O. Box 81608, San Diego, CA 92138
T. D. Gulden
K. S. Mazdiyasni
93. GENERAL MOTORS CORPORATION, Allison Gas Turbine Operations, Low
Heat Rejection Diesel Technology, P.O. Box 420, Indianapolis, IN
46206
H. E. Helms
- 94-95. GEORGIA INSTITUTE OF TECHNOLOGY, 225 North Avenue, Atlanta, GA
30332
W. J. Lackey
T. L. Starr
- 96-98. GTE LABORATORIES, INC., 40 Sylvan Road, Waltham, MA 02254
M. L. Huckabee
A. E. Pasto
V. Sarin
99. HUGHES AIRCRAFT COMPANY, P.O. Box 902, 2000 East El Segundo
Boulevard, El Segundo, CA 90245
Mike Gardos
100. KAMAN SCIENCES CORPORATION, 1500 Garden of the Gods Road,
P.O. Box 7463, Colorado Springs, CO 80933
J. L. Carr
101. KENNAMETAL, INC., P.O. Box 231, Latrobe, PA 15650
E. J. Oles

102. KRW ENERGY SYSTEMS, P.O. Box 158, Madison, PA 15663
C. A. Andersson, Jr.
- 103-105. LANXIDE CORPORATION, Tralee Industrial Park, Newark, DE 19711
V. Irick, Jr.
M. Newkirk
A. W. Urquhart
- 106-108. LAWRENCE BERKELEY LABORATORY, University of California,
P.O. Box 808, 1 Cyclotron Road, Berkeley, CA 94720
D. H. Boone
A. G. Evans
A. V. Levy
- 109-111. LOS ALAMOS NATIONAL LABORATORY, P.O. Box 1663, Los Alamos, NM
87545
F. D. Gac
G. F. Hurley
J. J. Petrovic
- 112-113. MARTIN MARIETTA LABORATORIES, 1450 South Rolling Road,
Baltimore, MD 21227
D. C. Nagle
A. R. C. Westwood
- 114-115. MASSACHUSETTS INSTITUTE OF TECHNOLOGY, Cambridge, MA 02139
H. K. Bowen
J. S. Haggerty
- 116-117. MECHANICAL TECHNOLOGY, INC., 968 Albany-Shaker Road,
Latham, NY 12110
W. F. Bessler
M. Schreiner
118. NASA-LANGLEY RESEARCH CENTER, MS 188-B, Hampton, VA 23665
D. R. Tenney
- 119-124. NASA-LEWIS RESEARCH CENTER, 21000 Brookpark Road, Cleveland, OH
44135
C. C. Berndt
D. H. Buckley
S. R. Levine
T. J. Miller
H. B. Probst
Harold Sliney

125. NATIONAL ACADEMY OF SCIENCES, National Materials Advisory Board,
Washington, DC 20418
R. M. Spriggs
- 126-127. NATIONAL BUREAU OF STANDARDS, 562 Fracture and Deformation,
Gaithersburg, MD 20899
E. R. Fuller
S. M. Wiederhorn
- 128-129. NORTH CAROLINA STATE UNIVERSITY, Department of Materials
Engineering, P.O. Box 5427, 232 Riddick Laboratory, Raleigh,
NC 27607
Hans Conrad
R. F. Davis
130. NORTH CAROLINA STATE UNIVERSITY, P.O. Box 5995, Raleigh, NC 27607
H. Palmour III
131. OAK RIDGE ASSOCIATED UNIVERSITIES LIBRARY, Oak Ridge, TN 37831
MERT Division
132. OHIO STATE UNIVERSITY, 2041 College Road, Columbus, OH 43210
Dennis Readey
- 133-134. PENNSYLVANIA STATE UNIVERSITY, Materials Engineering Research
Laboratory, 201 Steidle Building, University Park, PA 16802
Karl Spear
R. E. Tressler
- 135-137. PRATT & WHITNEY AIRCRAFT, 400 Main St., East Hartford, CT 06108
O. Chen
C. S. Giggins
D. L. Ruckle
- 138-139. ROCKWELL INTERNATIONAL, 1049 Camino Dos Rios, P.O. Box 1085,
Thousand Oaks, CA 91360
F. F. Lange
P. E. D. Morgan
140. RUTGERS UNIVERSITY, P.O. Box 909, Bowser Road, Piscataway, NJ 08854
J. B. Wachtman, Jr.
141. SAN FERNANDO LABORATORIES, 10258 Norris Avenue, Pacoima, CA
91331
R. A. Holzl

142. SANDIA NATIONAL LABORATORIES, P.O. Box 5800, Albuquerque, NM
87115
Donald Maddox
143. R. L. Smith, P.O. Box 98, Chassel, MI 49916
144. TECHNOLOGY ASSESSMENT AND TRANSFER COMPANY, 9607 Muirfield
Drive, Upper Marlboro, MD 20772
L. L. Fehrenbacher
145. 3M COMPANY, 3M Center, 218-35-04, St. Paul, MN 55144
R. E. Richards
146. UNION CARBIDE CORPORATION, Market Development, Carbon Products
Division, P.O. Box 6087, Cleveland, OH 44101
M. B. Dowell
147. U.S. ARMY TANK-AUTOMOTIVE COMMAND (TACOM), R&D Center,
Warren, MI 48090
P. C. Glance
- 148-149. U.S. DEPARTMENT OF DEFENSE, Advanced Research Projects Agency,
1400 Wilson Boulevard, Arlington, VA 22209
S. G. Wax
B. F. Wilcox
- 150-152. UNITED TECHNOLOGIES RESEARCH CENTER, Silver Lane, MS 24,
East Hartford, CT 06108
J. J. Brennan
Karl Prewo
E. R. Thompson
153. UNIVERSITY OF TENNESSEE, Department of Materials Science,
Knoxville, TN 37996
J. E. Spruill
- 154-155. UNIVERSITY OF WASHINGTON, Seattle, WA 98195
R. C. Bradt
J. I. Mueller
156. VIRGINIA POLYTECHNIC INSTITUTE AND STATE UNIVERSITY, Blacksburg,
VA 24061
D. P. H. Hasselman
157. VOUGHT CORPORATION, MSTH 83, P.O. Box 225907, Dallas, TX 75265
H. F. Volk

- 158-159. W. R. GRACE & COMPANY, 7379 Route 32, Columbia, MD 21044
R. W. Rice
J. P. Skalny
160. WESTINGHOUSE ELECTRIC CORPORATION, Research and Development Center, 1310 Beulah Road, Pittsburgh, PA 15235
R. J. Bratton
- 161-162. WILLIAMS INTERNATIONAL CORPORATION, 2280 West Maple Road, Walled Lake, MI 48088
William Chapman
Peter Nagy
163. DOE, ENERGY CONVERSION & UTILIZATION TECHNOLOGIES DIVISION, Route Symbol CE-142, Forrestal Building, Washington, DC 20545
J. J. Eberhardt
- 164-165. DOE, MORGANTOWN ENERGY TECHNOLOGY CENTER, P.O. Box 880, Morgantown, WV 26505
D. Dubis
J. S. Wilson
166. DOE, OAK RIDGE OPERATIONS OFFICE, P.O. Box E, Oak Ridge, TN 37831
Office of Assistant Manager for Energy Research and Development
167. DOE, OFFICE OF BASIC ENERGY SCIENCES, Division of Materials Sciences, ER-131, GTN, Washington, DC 20545
F. V. Nolfi
168. DOE, OFFICE OF FOSSIL ENERGY, FE-14, Mail Stop B127, GTN, Washington, DC 20545
F. M. Glaser
- 169-170. DOE, OFFICE OF VEHICLE AND ENGINE RESEARCH AND DEVELOPMENT, Forrestal Building, 1000 Independence Avenue, Washington, DC 20585
A. A. Chesnes
R. B. Schulz
171. DOE, PITTSBURGH ENERGY TECHNOLOGY CENTER, P.O. Box 10940, Pittsburgh, PA 15236
S. W. Chun

172-201. DOE, TECHNICAL INFORMATION CENTER, Office of Information Services,
P.O. Box 62, Oak Ridge, TN 37831

For distribution by microfiche as shown in DOE/TIC-4500,
Distribution Categories UC-90c (Coal Conversion and
Utilization-Coal Gasification), UC-90e (Coal Conversion and
Utilization-Direct Combustion of Coal), UC-90h (Coal
Conversion and Utilization-Materials and Components), UC-93
(Energy Conversion), UC-95 (Energy Conservation), and UC-96
(Energy Conservation-Transportation).